Excitation and decay of vibrational autodetaching states of N_2^- produced in collisions of H^- with N_2

John S. Risley

Department of Physics, North Carolina State University, Raleigh, North Carolina 27607 and Department of Physics, University of Washington, Seattle, Washington 98195*

(Received 6 June 1977; revised manuscript received 10 August 1977)

A significant perturbation in the energy distribution of electrons has been observed for collisions of H^- on N_2. The spacings between the large oscillations in the 1- to 4-eV region of the ejected electron spectra have been measured at observation angles between 30° and 150° for impact of 35- to 10000-eV H^- on N_2. A model is proposed which interprets these results in terms of the formation and decay of a series of vibrational autodetaching states of N_2^-. Electron distributions calculated using a molecular model based on the Franck-Condon principle for the excitation of the N_2^- states and various possibilities for the decay are compared with the experimental results.

I. INTRODUCTION

Previously, we reported the observation of a significant perturbation in the intensity of low-energy secondary electrons produced in collisions of H^- with N_2.[1,2] The structure, consisting of a number of oscillations in the electron energy distribution between 1 and 4 eV, was attributed to vibrational autodetaching states of N_2^-. This paper reports new measurements both for lower collision energies and larger observation angles. The energy separation between each line has been measured. Using these results, a model is proposed for the formation and decay of molecular N_2^- vibrational states.

Until the present experiments, evidence for the low-lying N_2^- states came from resonant structure in low-energy electron scattering measurements: (i) the total vibrational excitation cross sections,[3,4] (ii) total scattering cross sections,[5-8] (iii) electron loss cross sections at forward angles,[9-11] and (iv) elastic and inelastic differential cross sections.[12-16] The resonances have been interpreted as compound states of N_2^- using phenomenological theories with adjustable parameters[17-22] and fundamental, *ab initio* calculations.[23,24]

Although the correspondence between a resonance in electron scattering cross sections and an excited state of the negative ion is well understood, there are few similarities in the formation of the N_2^- states by electron impact and by charge transfer in negative-ion impact. However, the two collision techniques complement one another. Negative-ion collisions produce an emission spectrum of N_2^-, while electron collisions produce an absorption spectrum of N_2. Thus for H^- collisions the evidence for the N_2^- states bears only slight resemblance to the results from electron impact data. The proposed reaction of H^- with N_2 is

$$H^- + N_2(0) \rightarrow H + N_2^-(\nu^-)$$

and then

$$N_2^-(\nu^-) \rightarrow N_2(\nu) + e^- .$$

The method reported here for observing vibrational excitation of molecules may prove to be important in our understanding of low-energy excitation to vibrational states in ion-molecule or atom-molecule collisions. Techniques available for direct observation of the excited vibrational states of diatomic molecules are not practical in the laboratory because of the experimental difficulties in detecting infrared radiation and because of the long lifetime of the vibrational states of homonuclear molecules. Energy loss of ionic projectiles is another technique which could provide complementary data on vibrational excitation of molecules.

II. EXPERIMENTAL RESULTS

The apparatus used in these measurements has been described previously.[25-27] Briefly, H^- ions were directly extracted from a duoplasmatron ion source, focused into a beam, and magnetically analyzed before passing into a cylindrical cell containing the N_2 target gas at a pressure of about 5×10^{-4} Torr. A long Faraday cup and tube containing the last beam collimator extended into the gas cell.

A parallel-plate electrostatic analyzer was mounted on a rotatable platform outside the gas cell which enabled us to make measurements at angles continuously from 30° to 150°. The front electrode of the analyzer was held at zero potential so that the transmission of the analyzer was directly proportional to the kinetic energy of the

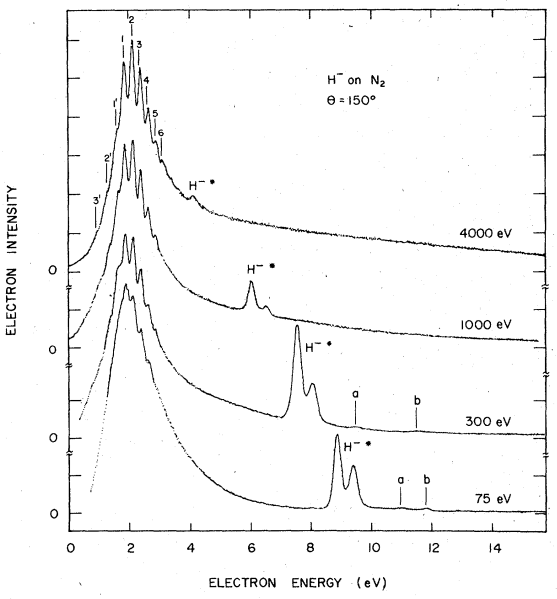

FIG. 1. Energy distribution of secondary electrons produced in collisions of H^- with N_2 observed at 150°. H^- lines are shifted in the laboratory reference frame because of reaction kinematics; see Ref. 25.

electrons.

The magnetic field in the region of the analyzer was annulled to less than 20 mG with Helmholtz coils. Electric fields arising from differences in contact potential were reduced by coating the surfaces of the gas cell and analyzer with acetylene black. The coating also helped absorb scattered, low-energy background electrons.

Figure 1 shows electron spectra at 150° for four representative collision energies of H^- between 75 and 4000 eV. Six distinct lines, labeled 1–6, are found in the electron energy range between 2 and 4 eV. Below 2 eV there are three shoulders labeled 1′–3′. The intensity of the electrons was not corrected for the transmission function of the parallel-plate electrostatic analyzer which varies linearly with the kinetic energy of the electrons. Below 2 eV the intensity of electrons may have been severely attenuated by small, residual electric and magnetic fields within the analyzer and scattering cell which were not eliminated using the precautions mentioned above.

Above 4 eV, lines attributable to autodetaching states of H^- are observed which are shifted in the laboratory reference frame because of reaction kinematics.[25] The structure labeled *a* arises from H^- states lying below the $n=3$ level, whereas the intense lines at lower energy originate from H^- states below the $n=2$ level. The structure labeled *b* is tentatively identified with decays from the core-excited Feshbach states of N_2^-.[16] Higher-resolution scans are needed for more positive identification.

Figure 2 shows electron spectra observed at forward angles for collision energies of H^- between 1 and 10 keV. As in Fig. 1, six to seven distinct lines are found between 2 and 4 eV. As the collision energy increases (6–10 keV) the oscillations are not as apparent, owing to the increase of a broad peak in the continuum or background electrons located at an electron velocity roughly equal to the H^- ion velocity.

Comparison of the relative intensity of the lines reveals, for fixed H^- energy, no noticeable change for different observation angles from 30° to 150°, except that caused by the continuum electrons. Since the N_2^- states have been identified with a shape resonance of a symmetry $^2\Pi_g$, isotropy in the intensity implies there is no preferential population of each magnetic substate of the total angular momentum with respect to the ion-beam axis; that is, for H^- collisions the ion-beam axis is not a "good" axis of quantization.

For fixed observation angle the relative intensity of each line changes as the collision energy is

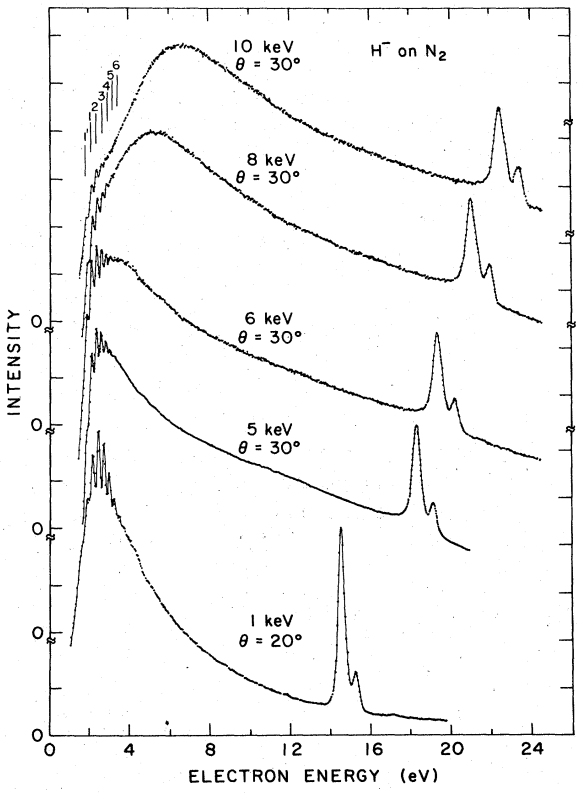

FIG. 2. Energy distribution of secondary electrons produced in collisions of H^- with N_2 observed at forward angles.

TABLE I. Energy separations between the low-lying peaks and shoulders.

Structure	Energy (eV)
2′-3′	0.29 ± 0.03
1′-2′	0.31 ± 0.03
1-1′	0.23 ± 0.03
2-1	0.26 ± 0.02
3-2	0.26 ± 0.01
4-3	0.25 ± 0.01
5-4	0.24 ± 0.02
6-5	0.23 ± 0.02

increased. For collision energies between 35 and 1000 eV, the valleys between the peaks increase, the discernible number of lines increases from four to seven, and the number of shoulders increases from one to three. From 4 to 10 keV the number of discernible oscillations starts to decrease from seven to four. This result may be caused by the large intensity of secondary electrons.

To within experimental uncertainty, the spacings between each line were not dependent on the collision energy or observation angle. Table I lists the energy separation between each line obtained from an average of measurements of the electron spectra for H^- collision energies from 75 to 10 000 eV and observation angles at 30°, 90°, and 150°. The separations above peak 1′ are roughly the same as the spacings between the vibrational levels of N_2^- (0.24 eV), consistent with electron scattering measurements, and below peak 1′ they are roughly the same as the N_2 levels (0.29 eV). The position of peak 1 was 2.0 ± 0.3 eV. The full width at half maximum (FWHM) of each line was approximately 0.2 eV. The analyzer resolution was about 0.05–0.07 eV.

III. DISCUSSION

A possible electron transfer reaction involving H^- with N_2 is shown in Fig. 3(b) using a molecular model for N_2^-.[17-23] In this example N_2 in the ground state is excited to $\nu^- = 3$ of N_2^-. The $N_2^-(3)$ state can decay to each energetically allowed vibrational state of $N_2(\nu)$ with a certain branching ratio. If decay occurs to the ground state, an electron with a kinetic energy of 2.62 eV is emitted. If decay occurs to an excited vibrational level of $N_2(\nu)$, an electron is emitted with a kinetic energy less than 2.62 eV. A series of lines will result with a spacing equal to the vibrational levels of N_2. The lowest kinetic energy of the autodetaching electron, in this example, is less than 0.13 eV for a decay to $\nu = 9$ of N_2.

On the other hand, if each N_2^- state decayed only to the ground state of N_2, a series of lines would result with a spacing equal to the vibrational levels of N_2^-, about 0.24 eV. The energy of the lowest-lying line would be 1.89 eV.

To test various excitation and decay possibilities, a model was developed for the expected electron energy distribution. Before proposing a specific model several general features of the ejected spectra should be noted: (a) Well-defined structure exists above 3.0 eV, for example, peak 6, (b) the oscillations are more pronounced above 2.0 eV than below, (c) the relative intensity of each oscillation exhibits little change as the H^- collision energy is varied by two orders of magnitude, and (d) the relative separation between each line remains constant regardless of observation angle or collision energy (75–10 000 eV).

Thus, the model must give rise to ejection of high-energy electrons with respect to the N_2-N_2^- system. In addition, because of lack of the usual characteristics of interference effects, that is, rapid variation of the spectral features with collision velocity or observation angle, the relative phase difference in the amplitudes for exciting each N_2^- state may not be important (in contradiction with electron scattering). In other words, we observe experimentally an averaging of the relative phase in exciting the upper N_2^- states.

With these ideas as a basis, an expression for the electron intensity, as observed with our analyzer, can be written as being proportional to

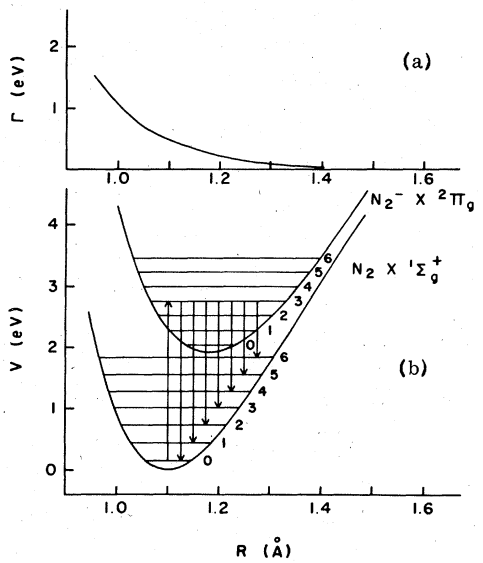

FIG. 3. Potential energy curves for the N_2-N_2^- system showing one excitation transition to $\nu^- = 3$ and subsequent decay channels.

$$\sum_{\nu^-=0}^{6}\sum_{\nu=0}^{6}\sigma(\nu^-)\gamma(\nu^-,\nu)EL(E), \tag{1}$$

where $\sigma(\nu^-)$ is the cross section for exciting the ν^- state of N_2^- from the ground state N_2; $\gamma(\nu^-,\nu)$ is the branching ratio of the upper $N_2^-(\nu^-)$ state to the lower $N_2(\nu)$ state; E, which is equal to the kinetic energy of the electron, accounts for the transmission factor of our electrostatic analyzer at high energies; and $L(E)$ is the usual Lorentzian line profile:

$$L(E)=\frac{\frac{1}{4}\Gamma^2}{[E-\Delta E(\nu^-,\nu)]^2+\frac{1}{4}\Gamma^2}, \tag{2}$$

where $\Delta E(\nu^-,\nu)$ is the difference between the $N_2^-(\nu^-)$ energy level and the $N_2(\nu)$ level. Γ is the effective or average FWHM for the N_2^- state. For comparative purposes we adjusted Γ to give the best fit with data. Unless stated otherwise, $\Gamma=0.2$ eV. Only vibrational levels below seven were considered.

Because the relative intensities of each line did not change with collision velocity and because the energy transfer was small compared with the collision energy, it was assumed that electron transfer to the N_2^- state could be described in terms of a fast or sudden transition. Therefore the Franck-Condon principle was invoked to yield

$$\sigma(\nu^-)=|a(\nu^-)|^2\left|\int\psi_\nu-\psi_0 dR\right|^2, \tag{3}$$

where $a(\nu^-)$, the transition amplitude for all the electrons from the initial H^-+N_2 state to the final $H+N_2^-$ state, is assumed not to depend strongly on ν^- and set equal to a constant value. $|\int\psi_\nu-\psi_0 dR|^2$ is the Franck-Condon factor (FCF) or overlap integral squared of the nuclear vibrational wave functions for $N_2^-(\nu^-)$ and $N_2(0)$.

The wave functions ψ are those for a Morse potential and were computed using a procedure outlined by Nicholls.[28] The Morse potential can be written as

$$E(R)=D_e(1-e^{-(R-R_0)/a})^2. \tag{4}$$

The energy levels are given approximately by

$$E_\nu=\omega_e(\nu+\tfrac{1}{2})-\omega_e x_e(\nu+\tfrac{1}{2})^2. \tag{5}$$

The following parameters[29] were used:

	N_2	N_2^-
D_e (eV)	9.90	11.96
R_0 (Å)	1.0977	1.1802
a (Å)	0.3720	0.49
ω_e (eV)	0.2923	0.244
$\omega_e x_e$ (eV)	0.001 75	0.001 24

The energy difference between the minimum of the N_2 and N_2^- potential curves is $E^-(R_0^-)-E(R_0)=1.912$ eV.

The Franck-Condon factors for the above potential parameters are listed in Table II. Although the potential parameters for the N_2 curve are known to high accuracy from optical spectroscopic data, the accuracy of the parameters for the N_2^- curve is not as high. Uncertainty in the equilibrium position R_0^- for N_2^-, an adjustable parameter in the electron scattering model,[29] can produce considerable uncertainty in those FCF's which are small because of the oscillatory nature of the overlapping wave functions. However, since those FCF's which are larger than about 0.1 are not affected strongly by an uncertainty in R_0^-, the general features of the excitation cross section can be noted. From Table II it can be seen that excitation is most probable to $\nu^-=1$, followed by $\nu^-=2$ and 0. Excitation to $\nu^-=5$ and 6 is roughly a factor of 10 smaller than to $\nu^-=1$.

Since the branching ratio $\gamma(\nu^-,\nu)$ for the upper state $N_2^-(\nu^-)$ to the lower state $N_2(\nu)$ is not readily available from existing calculations,[17-24] three different possibilities were considered. The ratio which incorporates conventional molecular principles is

$$\gamma_1(\nu^-,\nu)=\left(\Delta E(\nu^-,\nu)^{5/2}\Big/\sum_{\nu=0}^{n}\Delta E(\nu^-,\nu)^{5/2}\right)\times\left|\int\psi_\nu-\psi_\nu dR\right|^2, \tag{6}$$

TABLE II. Franck-Condon factors for the lowest-lying N_2-N_2^- ($^2\Pi_g$-$X\,^1\Sigma_g^+$) system. A number in parentheses is the power of 10 by which the preceding number is to be multiplied.

ν^- \ ν	0	1	2	3	4	5	6
0	2.22(−1)	3.68(−1)	2.67(−1)	1.10(−1)	2.85(−2)	4.72(−3)	4.98(−4)
1	3.05(−1)	5.51(−2)	6.67(−2)	2.56(−1)	2.13(−1)	8.41(−2)	1.87(−2)
2	2.35(−1)	2.59(−2)	1.68(−1)	4.64(−3)	1.25(−1)	2.44(−1)	1.47(−1)
3	1.34(−1)	1.36(−1)	2.38(−2)	1.08(−1)	7.32(−2)	2.59(−2)	2.08(−1)
4	6.34(−2)	1.65(−1)	2.01(−2)	9.58(−2)	2.37(−2)	1.23(−1)	3.75(−4)
5	2.62(−2)	1.23(−1)	9.95(−2)	4.82(−3)	1.08(−1)	6.35(−4)	1.14(−1)
6	9.77(−3)	7.04(−2)	1.29(−1)	2.74(−2)	4.591(−2)	6.76(−2)	2.76(−2)

TABLE III. $\gamma_2(\nu^-, \nu)$.

ν^- \ ν	0	1	2	3	4	5	6
0	0.41	0.27	0.17	0.092	0.042	0.014	0.0019
1	0.37	0.26	0.17	0.10	0.057	0.026	0.0081
2	0.34	0.25	0.17	0.11	0.068	0.037	0.016
3	0.32	0.24	0.17	0.12	0.076	0.046	0.024
4	0.29	0.23	0.17	0.12	0.083	0.054	0.032
5	0.27	0.22	0.16	0.12	0.087	0.060	0.038
6	0.26	0.21	0.16	0.12	0.090	0.065	0.044

where n is the highest vibrational level of N_2 to which the N_2^- state can decay. The term containing $\Delta E^{5/2}$ accounts for the penetrability of an outgoing electron with kinetic energy ΔE through the $l=2$ centrifugal barrier of the N_2^- potential.[30]

In using the FCF one assumes that the transition probability, which is proportional to $\Gamma(R)$, does not change rapidly with R over the region in which the overlap of the nuclear wave functions ψ_{ν^-} and ψ_ν is large.[31] From Fig. 3(a) it can be seen that $\Gamma(R)$ changes significantly in the region of R from 0.5 to 1.4 Å. However, in the region of large overlap, the variation in $\Gamma(R)$ is not sufficient to modify the FCF's appreciably; that is,

$$\int \psi_{\nu^-}\Gamma(R)^{1/2}\psi_\nu dR \approx \langle \Gamma^{1/2}\rangle \int \psi_{\nu^-}\psi_\nu dR\,, \tag{7}$$

where $\langle \Gamma^{1/2}\rangle$ is an average value of $\Gamma(R)$ independent of both ν^- and ν.

When invoking the Franck-Condon principle, one usually assumes the molecule will vibrate a large number of times before decaying to a lower state. For N_2^-, however, the transition probability is large; that is, the lifetime is on the order of one vibrational period.[16] The effect of such a large transition probability on the scattering of electrons by N_2 gave rise to the boomerang model by Herzenberg.[21,22] At present it is unclear how to adapt the details of the boomerang model to the H^- on N_2 problem.

Using a suggestion by Herzenberg[29] a branching ratio of the form

$$\gamma_2(\nu^-, \nu) = \Delta E(\nu^-, \nu)^{5/2} \Big/ \sum_{\nu=0}^{n} \Delta E(\nu^-, \nu)^{5/2} \tag{8}$$

was tested. Table III lists $\gamma_2(\nu^-, \nu)$.

The third decay scheme tested was one in which it was assumed that all of the states decayed only to the ground vibrational state of N_2, $\nu=0$:

$$\gamma_3(\nu^-, \nu) = \delta_{\nu 0}\,. \tag{9}$$

This assumption seemed reasonable based on the characteristics of the ejected electron spectra: lines starting at 1.9 eV and extending upward to above 3.5 eV, an average spacing of about 0.25 eV which is roughly the same as the spacing between adjacent vibrational levels in N_2^-, and the lack of strong features below 1.9 eV which, if present, would indicate significant population of the low-lying vibrational levels of N_2.

The results of calculating the electron distribution for the H^- on N_2 reaction using Eq. (1) and the three possible branching ratios, Eqs. (6), (8), and (9), are displayed in Figs. 4(c), 4(d), and 4(e), respectively. For comparative purposes, a typical experimental spectrum (4-keV H^- on N_2 observed at 150°) is shown in Fig. 4(a). We have adjusted the energy scale so that peak 1 lies at 1.9 eV. Since the model does not account for direct electron detachment, the experimental results are displayed in a slightly different fashion in Fig. 4(b), in which a continuous background [solid line in Fig. 4(a)] has been subtracted from the experimental spectrum. The background curve was estimated from continuum distributions based on H^- collisions with other gas targets which have no resonant structure in this energy region. Although the background subtraction procedure is ultimately quite

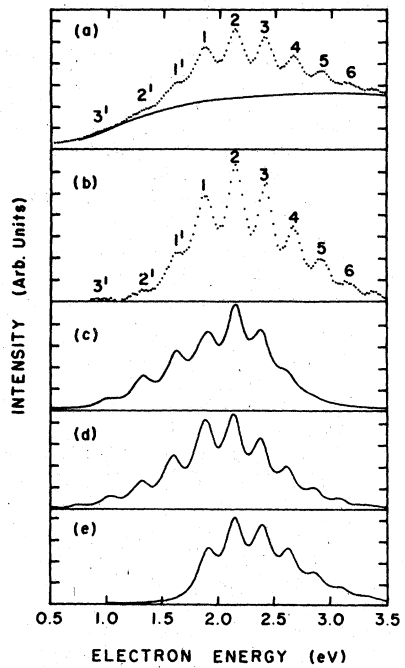

FIG. 4. Electron energy distribution from N_2^-: (a) experiment, 4-keV H^- on N_2 observed at 150°; (b) experiment, background subtracted from (a); (c) model, branching ratio proportional to $\Delta E^{5/2}\times$ FCF; (d) model, branching ratio proportional to $\Delta E^{5/2}$ with $\Gamma=0.15$ eV; (e) model, branching ratio equal to $\delta_{\nu 0}$. The energy scale for the experimental results has not been calibrated.

TABLE IV. Relative population of the lowest vibrational states of N_2. The branching ratio $\gamma_i(v^-, v)$ is defined in the text.

v	$\gamma_1(v^-, v)$	$\gamma_2(v^-, v)$	$\gamma_3(v^-, v)$
0	0.50	0.36	1
1	0.22	0.25	0
2	0.13	0.17	0
3	0.079	0.11	0
4	0.044	0.061	0
5	0.021	0.031	0
6	0.0087	0.013	0

arbitrary, it can be seen in Figs. 4(a) and 4(b) that it does not significantly affect the general characteristics of the structure.

By combining the expressions for the excitation cross section $\sigma(v^-)$ [see Eq. (3)] and the branching ratios $\gamma_i(v^-, v)$, it is possible to predict the relative populations $\sigma(v)$ of the N_2 vibrational states which are formed via the resonant or vibrational autodetaching process:

$$\sigma(v) = \sum_{v^-=0}^{6} \gamma(v^-, v)\sigma(v^-) . \tag{10}$$

Table IV lists the relative populations for v up to six, normalized to unity. For $\gamma_1(v^-, v)$ and $\gamma_2(v^-, v)$, the most populated state of N_2 is $v=0$ with the relative population decreasing monotonically with increasing v. For $\gamma_3(v^-, v)$, only the lowest state $v=0$ is populated. It would be of much interest to compare these population distributions with those arising from nonresonant excitation.

In general, the model calculations compare favorably with experiment. At present, though, we are unable to state which of the three branching ratio possibilities is valid. Decisive tests could be made by developing an electrostatic analyzer with known transmission characteristics below 2 eV and by accurately calibrating the energy scale to within ±0.05 eV. Furthermore, more theoretical work is needed on the important diatomic N_2^- molecule; specifically, the branching ratios should be calculated from first principles.

ACKNOWLEDGMENTS

The author wishes to thank Dr. Herzenberg for valuable comments and unpublished data regarding the parameters of the Morse potential for N_2^-, Dr. Nicholls, Dr. Macek, and Dr. Burke for helpful suggestions, and Dr. R. Geballe for continued support and encouragement. This work was supported in part by the National Science Foundation.

*Permanent address.
[1]J. S. Risley, in *Atomic Physics IV, Proceedings of the Fourth International Conference on Atomic Physics, Heidelberg, 1974,* edited by G. zu Putlitz, E. W. Weber, and A. Winnacker (Plenum, New York, 1975), pp. 487-528.
[2]J. S. Risley, in *Electronic and Atomic Collisions, Abstracts of Papers of the Ninth ICPEAC,* edited by J. S. Risley and R. Geballe (University of Washington, Seattle, 1975), pp. 880-881.
[3]R. Haas, Z. Phys. 148, 177 (1957).
[4]G. J. Schulz, Phys. Rev. 116, 1141 (1959).
[5]M. J. W. Boness and J. B. Hasted, Phys. Rev. Lett. 21, 526–528 (1966).
[6]D. E. Golden, Phys. Rev. Lett. 17, 847–848 (1966).
[7]D. E. Golden and H. Nakano, Phys. Rev. 144, 71–74 (1966).
[8]R. E. Kennerly and R. A. Bonham (private communication).
[9]G. J. Schulz, Phys. Rev. 125, 229–232 (1962).
[10]H. G. M. Heideman, G. E. Kuyatt, and G. E. Chamberlain, J. Chem. Phys. 44, 355–358 (1966).
[11]J. B. Hasted and A. M. Awan, J. Phys. B 2, 367 (1969).
[12]G. J. Schulz, Phys. Rev. 135, A988–A994 (1964).
[13]G. J. Schulz and H. C. Koons, J. Chem. Phys. 44, 1297 (1966).
[14]D. Andrick and H. Ehrhardt, Z. Phys. 192, 99–106 (1966).
[15]H. Ehrhardt and K. Willmann, Z. Phys. 204, 462–473 (1967).
[16]G. J. Schulz, Rev. Mod. Phys. 45, 423–486 (1973).
[17]A. Herzenberg and F. Mandl, Proc. R. Soc. London Ser. A 270, 48–71 (1962).
[18]J. C. Y. Chen, J. Chem. Phys. 40, 3507 (1964).
[19]J. C. Y. Chen, J. Chem. Phys. 40, 3513 (1964).
[20]J. C. Y. Chen, J. Chem. Phys. 45, 2710 (1966).
[21]A. Herzenberg, J. Phys. B 2, 548–558 (1968).
[22]D. T. Birtwistle and A. Herzenberg, J. Phys. B 4, 53–66 (1971).
[23]M. Krauss and F. H. Mies, Phys. Rev. A 1, 1592–1598 (1970).
[24]N. Chandra and A. Temkin, Phys. Rev. A 13, 188–203 (1976).
[25]J. S. Risley, A. K. Edwards, and R. Geballe, Phys. Rev. A 9, 1115–1129 (1974).
[26]J. S. Risley and R. Geballe, Phys. Rev. A 9, 2485–2495 (1974).
[27]J. S. Risley and R. Geballe, Phys. Rev. A 10, 2206–2217 (1974).
[28]R. W. Nicholls, J. Res. Natl. Bur. Stand. Sec. A 65, 451–460 (1961); and private communication.
[29]Parameters for the Morse potential for N_2 were taken from B. Rosen, *Données Spectroscopiques Relatives aux Molecules Diatomiques* (Pergamon, New York, 1970), p. 268, and for N_2^- from Ref. 22 and A. Herzenberg (private communication).
[30]T. Y. Wu and T. Ohmura, *Quantum Theory of Scattering* (Prentice-Hall, Englewood Cliffs, 1962), p. 441. The angular momentum of the outgoing electron is believed to be *d* wave; see Ref. 15.
[31]G. Herzberg, *Molecular Spectra and Molecular Structure. I. Spectra of Diatomic Molecules,* 2nd ed. (Van Nostrand Reinhold, New York, 1950), p. 200.